Relocation and Storage Assignment Strategies Evaluation in a Multiple-deep Tier-captive Automated Vehicles Storage and Retrieval System with Undetermined Retrieval Sequence

Jakob Marolt (jakob.marolt@um.si)
University of Maribor: Univerza v Mariboru https://orcid.org/0000-0001-8162-8163
Nenad Kosanić
University of Belgrade
Tone Lerher
University of Maribor

Research Article

Keywords: Automated Warehouses, Multiple-deep AVS/RS, Discrete event simulation, Relocation, Rearrangement, Performance Analysis

Posted Date: July 6th, 2021

DOI: https://doi.org/10.21203/rs.3.rs-603627/v1

Version of Record: A version of this preprint was published at The International Journal of Advanced Manufacturing Technology on October 15th, 2021. See the published version at https://doi.org/10.1007/s00170-021-08169-x.

Relocation and storage assignment strategies evaluation in a multiple-deep tier-captive automated vehicles storage and retrieval system with undetermined retrieval sequence

Jakob Marolt[a1], Nenad Kosanić[b], Tone Lerher[c]

[a,] *University of Maribor, Faculty of Logistics, Mariborska c. 7, SI-3000, Celje, Slovenia*

[b] *University of Belgrade, Faculty of Mechanical Engineering, Kraljice Marije 16, Belgrade, Serbia*

[c]*University of Maribor, Faculty of Mechanical Engineering, Smetanova 17, SI-2000, Maribor, Slovenia*

Abstract

This paper studies multiple-deep automated vehicle storage and retrieval systems (AVS/RS) known for their high throughput performance and flexibility. Compared to a single-deep system, multiple-deep AVS/RS has a better space area utilisation. However, a relocation cycle occurs, reducing the throughput performance whenever another stock-keeping unit (SKU) blocks a retrieving SKU. The SKU retrieval sequence is undetermined, meaning that the arrangement is unknown, and all SKUs have an equal probability of retrieval. In addition to the shuttle carrier, a satellite vehicle is attached to the shuttle carrier and is used to access storage locations in multiple depths. A discrete event simulation of multiple-deep AVS/RS with a tier captive shuttle carrier was developed. We focused on the dual command cycle time assessment of nine different storage and relocation assignment strategies combinations in the simulation model. The results of a simulation study for (i) Random, (ii) Depth-first and (iii) Nearest neighbour storage and relocation assignment strategies combinations are examined and benchmarked for five different AVS/RS case study configurations with the same number of storage locations. The results display that the fivefold and sixfold deep AVS/RS outperform systems with fewer depths by utilising Depth-first storage and Nearest neighbour relocation assignment strategies.

Keywords: Automated Warehouses; Multiple-deep AVS/RS; Discrete event simulation; Relocation; Rearrangement; Performance Analysis.

---

[1] Corresponding author. Tel.: + 386 3 428 5309
E-mail address: jakob.marolt@um.si (J. Marolt)

1 Introduction and Problem description

The emergence of E-commerce and the pronounced diversity of products are altering the retailer industry. In the last ten years, the most significant challenges are the growing trend to deliver small orders with a relatively broad range of products in the shortest possible time [1].

Traditional warehouses have difficulties in meeting these challenges. The most labour-intensive process in warehouses is order picking, which, in most cases, is done manually [2]. A warehouse worker, referred to as an 'order-picker,' is often confronted with inadequate ergonomic solutions at the workplace and high-precision work requirements. At the same time, the work of the order-picker usually takes place in several shifts. By automating warehouse processes (especially the order picking process), part of the order-picker's workload can be taken over by an automated warehouse solution.

Over the last two decades, warehouse automation has developed remarkably fast. Considerable progress has been made in the Automated Vehicle Storage and Retrieval system (AVS/RS) or Shuttle-Based Storage and Retrieval System (SBS/RS).

AVS/RS is designed to store and retrieve stock-keeping units (SKUs) such as pallets, boxes, or totes. The AVS/RS consists of lifts (elevators), shuttle carriers, and racking, in which SKUs are stored. The elevator's lifting table provides vertical movements by placing SKUs in buffers in front of the rack storage area. Automatic shuttle carriers ensure storage and retrieval of SKUs in the horizontal direction of the storage rack. Compared to conventional crane-based Automated Storage and Retrieval Systems (AS/RS), AVS/RS has a higher throughput capacity, is more flexible, and has lower energy consumption per unit of throughput capacity [3].

The bottleneck in AVS/RS is the elevator, as the elevator has to serve several shuttle carriers located on different tiers of the storage rack [4]. As a result, shuttle carriers have lower utilisation as they remain in a neutral ('idle') mode for most of their operation. The utilisation of shuttle carriers can be improved by increasing the number of storage locations available in the AVS/RS system. The storage capacity can be expanded by adding more columns. However, the ratio between the storage area and the aisle area remains the same. Much better space area utilisation is achieved by adding more storage locations in-depth, perpendicular to the aisle (Figure 1).

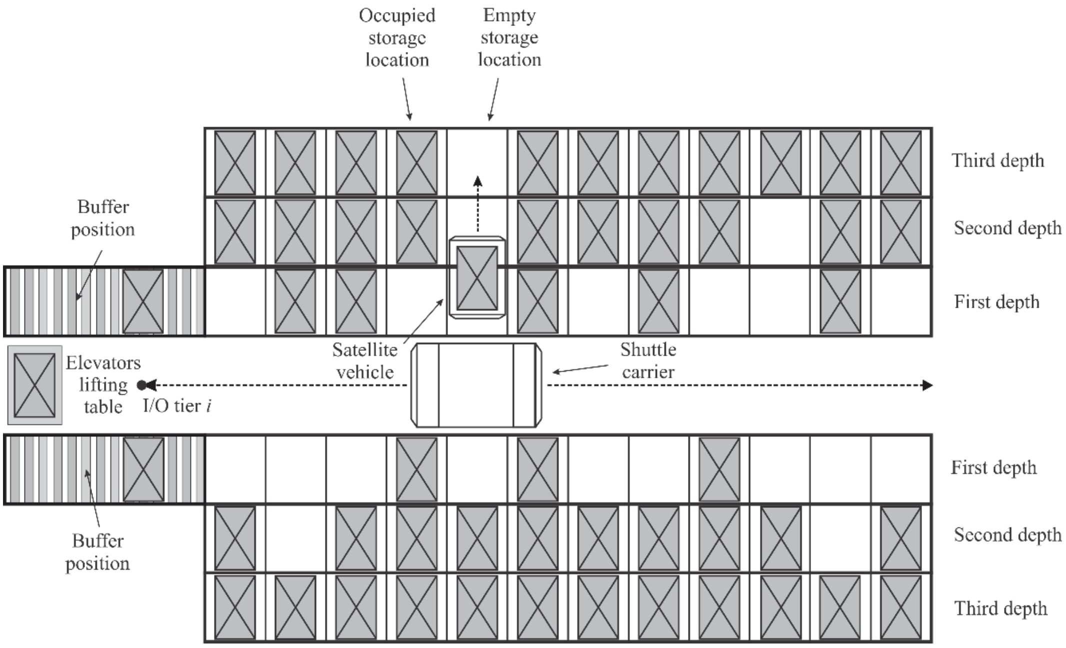

Figure 1: Floor of a triple-deep AVS/RS

By increasing the storage rack's depth, the space area utilisation of the storage rack is improved with a higher density of storage locations. But with multiple depths, relocation problems occur due to possible SKU blockages throughout the retrieval process. The SKU must be relocated if it blocks access to the ordered (retrieving) SKU. Relocation problem only occurs if there are SKUs with different products in the same lane or the FIFO (First-in-First-out) storage policy is applied. Each relocation represents an additional manipulation for the shuttle carrier, which negatively affects the throughput capacity of the AVS/RS. The new storage location of the blocked SKU must be reasonably selected to allow the AVS/RS system to maintain the maximum possible throughput capacity in future operation.

The aim of this research paper is to evaluate and compare the throughput performance of several combinations of storage and relocation assignment strategies for multiple-deep AVS/RS with tier-captive shuttle carrier. In this paper, only an undetermined dispatch problem is considered, where no information is given about the retrieval order of SKUs. When dispatch order is known partly or entirely in advance (determined dispatch problem), the SKU relocation and storage locations can be selected more efficiently through minimisation of necessary relocations in the future.

This paper is organised as follows. Section two (2) presents a literature review of double- and multiple-deep AVS/RS, focusing on storage and relocation assignment strategies. In section three (3) methodology is described. In Section four (4), simulation input parameters, the results of a case study and storage and relocation assignment strategies benchmark are presented. In the last section (5), the conclusions are made along with a proposal for future work.

2 Literature review

Even though in this paper, we studied AVS/RS, we also summarised some important publications regarding other automatic storage systems, which have made an essential contribution to our research problem. Based on the selected kinematic parameters of the storage and retrieval machine (S/R machine) and the storage rack configuration, the authors present analytical models for calculating the considered storage system's cycle times and, thus, the storage system's throughput capacity.

In 2002, Malmborg was the first who introduced the AVS/RS as an alternative to known crane-based AS/RS [3]. The author developed analytical models for estimating the AVS/RS throughput capacity and compared its performance with existing analytical models of crane-based AS/RS. He also proved that AVS/RS achieves higher throughput capacity and higher flexibility compared to crane-based AS/RS. A year later, Malmborg published the extension of his research work from 2002 and propose a model for estimating throughput capacity based on predicting the proportion of Dual Command (DC) cycles in AVS/RS [5]. A DC cycle is carried out when the shuttle carrier first stores an inbound SKU and retrieves outbound SKU without returning to the buffer location. His model for estimating the proportion of DC cycles was later used several times in the literature to calculate the throughput of various automated storage systems [4], [6]–[8]. In 2009 Roodbergen and Vis published a detailed overview article about crane-based AS/RS warehouse systems, and their results can also be generalised and applied to AVS/RS [9]. The article summarises publications from the last 30 years. They found that most researchers looked at a static rather than a dynamic storage system, where the storage and SKU shipping requirements were not constant over time. They also pointed out a shortage of storage assignment policies of non-traditional AS/RS.

In 2010 Lerher et al. considered the crane-based AS/RS storage system with two depths [4]. They proposed an analytical model to calculate the Single Command (SC) time and DC cycles to calculate the storage system's throughput capacity. A relocation problem is included in the model employing a relocation assignment strategy to the nearest free storage location (nearest neighbour). Marchet et al. developed an analytical model based on server systems for a single depth AVS/RS [10]. Carlo and Vis discussed the classification of operations (planning problem) of a special implementation of the AVS/RS with one lift with two separate lifting tables that do not overlap [11]. Roy et al. examined the occurrence of a (possible) blockade of shuttle carriers in AVS/RS when several shuttle carriers work on the same floor of a rack storage area [12]. This type of AVS/RS is known as non-tier-captive systems. In 2015, Xu et al. were the first to consider two depths for a crane-based AS/RS with a dual-shuttle that can transport two SKUs in a single route [6]. They emphasised the importance of high space utilisation with additional depth in the AS/RS. Their paper presented an analytical model for the calculation of a Quadruple Command (QC) cycle for the specified type of storage system with double-deep AS/RS. They used a random storage assignment policy for the storage operation. During the relocation cycle, depending on the availability of the slots on the hoisted carriage, two scenarios could occur. If both slots were available, the SKU was relocated without placing the blocking SKU to a new storage location. However, if only one slot of the hoisted carriage was available, the SKU was relocated using the nearest neighbour assignment strategy.

The authors Ning et al. developed a simulation model for the parametric analysis of a single-depth AVS/RS that includes 81 different storage alternatives for a superior selection of AVS/RS [13]. The VDI Association (The association of German engineers) has submitted recommendations for a single depth AVS/RS [14]. Although VDI Recommendations 2692 stated that SKU relocation problems could occur in multiple depth storage systems, they did not include a detailed description nor suggested what relocation assignment strategy should be applied. In 2016, Lerher et al. presented an analytical model for determining SC and DC cycle times for a double-deep SBS/RS [7]. Due to applying a double-deep storage rack, a relocation problem may occur during an SKU retrieval. The relocation assignment strategy used is based on standard FEM 9.851, which relocates SKUs to the closest available empty location (nearest neighbour). Manzini et al. published a paper dealing with AVS/RS with multiple depths [15]. In their work, they restricted themselves to the selected product type on each floor of the storage rack, thus avoiding the problem of relocation. Analytical models were presented to determine the AVS/RS throughput performance. The efficiency of the proposed model was verified with a simulation model.

The European Materials Handling Federation (FEM) proposed a model for determining the cycle time and throughput capacity for a single and double-deep AVS/RS [16]. FEM 9.860 suggest the use of the nearest neighbour (NN) relocation assignment strategy. However, a multiple-deep AVS/RS is not considered in the standard. Ekren, 2017 presented a solution with 294 different single-deep AVS/RS simulations using queuing theory [8]. The utilisation of the elevators, the operating cycle time, and the AVS/RS throughput capacity can be observed by changing the number of entry/exit positions of the storage rack, aisles, and storage locations. The proposed solution allows for simultaneous assessment of many different configurations and an evaluation of the AVS/RS expected throughput capacity.

D’Antonio et al. presented an analytical model for a multiple-deep AVS/RS. A new subsystem in the AVS/RS was proposed to transport SKUs at deeper locations called a 'satellite vehicle' [17]. Similar to the work of Manzini et al., only products of the same type were stored in one storage depth. Because of this restriction, the problem of relocation was not considered. The retrieval operation of SKUs was following (Last-in-First-out) LIFO storage policy. In 2019, D'Antonio and Chabert expanded their previous work with a multiple-deep AVS/RS system that allows shuttle carriers to move from one tier of the storage tack to another [18]. They proposed a new analytical model for calculating the throughput capacity of a DC cycle. Since the other constraints remained the same, the relocation problem was not considered. The authors Boywitz and Boysen investigated the problem of storing frozen products in a warehouse with several depths [19]. Each product in the warehouse had a predetermined shipping time in the form of a 'due date window' that had to be fulfilled. For the storage process, they proposed a robust storage assignment policy, which is based on a mathematical model. They also studied the relocation problem during the product retrieval, but the blocking product was returned to the same location and not relocated to another storage location, as is the case in our paper.

In 2019, Authors Ha and Chae presented a decision model for determining the number of shuttle carriers in a single-deep AVS/RS [20]. Shuttle carriers can travel on different tiers by using an elevator. Wang et al. discussed a double-deep AVS/RS [21]. They assumed that the SKU dispatch order is not predetermined but that each SKU has a predefined time window in which it must also be retrieved. The retrieval of SKUs is partly deterministic. They posed the problem of order batching to achieve the highest possible throughput capacity of the AVS/RS.

In 2020, the author Eder published a paper studying a multiple-deep AVS/RS. He presented a method to determine the throughput capacity of the AVS/RS based on the open queuing network methodology [22]. Eder considered a random assignment strategy for storage operation and a nearest neighbour assignment strategy for a relocation operation. The proposed analytical model was verified by a discrete events simulation.

After a detailed review of the scientific literature focusing on multiple-deep AVS/RS, only a few scientific papers dealt with double or deep storage systems, Table 1.

Table 1: Research papers considering double or multiple-depth storage systems

Research paper	**Retrieval sequence information**	**Considered depth**	**Storage assignment strategy**	**Relocation assignment strategy**	**Type of storage system**
Lerher et al. (2010)	Undetermined	Double-deep	Random	Nearest neighbour	AS/RS
Xu et al. (2015)	Undetermined	Double-deep	Random	Nearest neighbour and utilisation of the shuttle's second slot	Dual shuttle AS/RS
Xu et al. (2018)	Undetermined	Multiple-deep	Random, Class-based (turnover based)	Returning to the I/O point rule	AS/RS
Lerher (2016)	Undetermined	Double-deep	Random	Nearest neighbour	SBS/RS
Manzini et al. (2016)	Undetermined	Multiple-deep	Random	/	AVS/RS
D'Antonio et al. (2018)	Undetermined	Multiple-deep	Random, Closest floor (CF), Closest channel (CC)	/	AVS/RS

Boywitz and Boysen (2018)	Known due dates	Multiple-deep	A robust storage assignment	Rearrangement to the same stack, after the retrieval	Deep-lane storage system
D'Antonio and Chiabert (2019)	Undetermined	Multiple-deep	Random, Closest floor (CF), Closest channel (CC)	/	AVS/RS
Guerrazzi (2019)	Undetermined	Multiple-deep	First, try to store to a non-full channel containing ULs of the same type. Else, store in an empty channel	/	AVS/RS
Wang et al. (2019)	Determined	Double-deep	/	Nearest neighbour	Multiple-tier shuttle system
Wang et al. (2020)	Undetermined	Multiple-deep	Random	/	Autonomous shuttle and stacker crane (AS/SC)
Eder (2020)	Undetermined	Multiple-deep	Random	Nearest neighbour	Tier-captive SBS/RS

Note: In the literature review, we also included other multiple-deep storage systems because we wanted to discover all different storage and relocation assignment strategies that were utilised.

Generally, the researchers developed analytical models that enable calculating the storage system's cycle time and throughput capacity. However, the analytical models are, in most cases, limited to selected storage and relocation assignment strategies (typically, random for storage and nearest neighbour for relocation process). In some cases, a numerical simulation was used for the verification of the analytical models. Only two scientific papers assumed some (partial) information of SKU shipping sequence [19], [21]. The rest were studying storage systems with undetermined SKU retrieval sequence. None of the reviewed research papers assessed different storage and relocation assignment strategies combinations on the studied storage system's performance.

Our study differs from the reviewed papers by (i) proposal of a Depth-first assignment strategy along with two well-established ones (Random and Nearest Neighbour); (ii) merging the assignment strategies into nine (9) storage and relocation assignment strategies combinations; (iii) evaluating their performance on five (5) different AVS/RS configurations with the same number of storage locations (by altering depth (D) and columns (C) of AVS/RS); and (iv) creating a benchmark comparison analysis of the storage and relocation assignment strategies combinations.

3 Methodology

In continuation, basic assumptions and notations will be introduced.

3.1 Assumptions and notations

Regarding the multiple-deep AVS/RS studied in this paper, the following main assumptions were considered:

- The shuttle carrier operated exclusively in the DC cycle. There are two reasons for this assumption. Firstly, the shuttle carrier performs more efficiently as it operates with fewer empty travels compared to an SC cycle. Secondly, after many iterations, the fill-grade factor (occupancy of the AVS/RS) remains the same.
- The lift was not considered in the simulation model, as this paper focuses on analysing the efficiency of a shuttle carrier's storage and relocation strategies in a tier-captive AVS/RS.
- There is always storage and a retrieval order in the order queue. With this notion, the AVS/RS is fully utilised during the simulation.
- The shuttle carrier is attached with a satellite vehicle that can move in-depth for reaching SKUs.
- The shuttle carrier and the satellite vehicle are working accordingly to the kinematic model proposed in chapter 3.4.
- The cycle time of the satellite vehicle is associated with the loading and unloading times of SKUs.
- The shuttle carrier and the satellite vehicle can carry one SKU only.
- Dwell point strategy: The shuttle carrier's starting point is at the buffer position of the i^{th} tier of the storage rack.

- The throughput performance in other tiers is equivalent to the analysed i^{th} tier.
- AVS/RS considered is tier-captive, meaning that shuttle carrier can't leave its tier.
- The blocking SKUs can't be relocated to another tier of AVS/RS.
- The AVS/RS consists of two sides of the storage rack with an aisle in the middle. The configuration of storage locations is symmetrical. The storage rack is composed of a number of columns (C) in the horizontal (x) direction, a number of depths (D) in the horizontal (y) direction and a number of tiers (T) in the vertical (z) direction.
- Only one SKU can fit in one storage location.
- The I/O point of the SKU is at the buffer location (Figure 1). There are two buffer locations on each side of the AVS/RS. One buffer location handles inbound SKUs and the other handles outbound SKUs.
- The retrieval SKU is selected by a random function (all SKUs have the same probability of being selected).
- The storage locations for inbound SKU and relocation locations for blocking SKU are selected based on the assignment strategy. In this paper, three different assignment strategies are considered: random, nearest neighbour and depth-first.

Operational parameters

$\boldsymbol{\alpha}$	Fill grade factor-alpha
$\boldsymbol{a}$	Acceleration/deceleration
$\boldsymbol{a_x}$	Acceleration of a shuttle carrier alongside columns (x-direction)
$\boldsymbol{a_y}$	Acceleration of a satellite vehicle in depth (y-direction)
$\boldsymbol{A_{aisle}}$	AVS/RS shuttle carrier's aisle area
$\boldsymbol{A_{storage}}$	AVS/RS storage area
$\boldsymbol{c}$	Index of a storage location (column)
$\boldsymbol{c_s}$	Start column
$\boldsymbol{c_{shuttle}}$	Shuttle column position
$\boldsymbol{c_d}$	Designated column

$\boldsymbol{C}$	Number of columns (storage locations alongside corridor)
$\boldsymbol{d}$	Index of a storage location (depth)
$\boldsymbol{d_d}$	Designated depth
$\boldsymbol{D}$	Number of depths in the storage system
$\boldsymbol{l_0}$	Distance between SKU buffer and first storage location (x-direction)
$\boldsymbol{l_{SKU}}$	Length of an SKU
$\boldsymbol{l_{ss}}$	Length of a storage location (x-direction)
$\boldsymbol{N}$	Number of storage locations in the AVS/RS
$\boldsymbol{N_{os}}$	Number of SKUs in the AVS/RS (occupied storage locations)
$\boldsymbol{N_{es}}$	Number of empty storage locations in the AVS/RS
$\boldsymbol{\omega_{rel}}$	Relocation frequency
$\boldsymbol{s}$	Path
$\boldsymbol{s_{critical}}$	Critical path when a vehicle reaches maximum velocity
$\boldsymbol{s_{SKU}}$	Side of the ordered (retrieving) SKU
$\boldsymbol{t_{depth}}$	Total depth time of a satellite vehicle
$\boldsymbol{t_{in/out}}$	Time of a satellite vehicle travelling in or out in-depth (y-direction)
$\boldsymbol{t_{load/unload}}$	SKU loading or unloading time by a satellite vehicle
$\boldsymbol{T_{buf}}$	Buffer travelling time in-depth
$\boldsymbol{T_{DC}}$	Cycle time of a dual command cycle
$\boldsymbol{T_{et}}$	Empty travel time of a dual command cycle
$\boldsymbol{T_{sto}}$	Storage operation time of a dual command cycle
$\boldsymbol{T_{sto-x}}$	Shuttle's carrier storage time (x-direction)
$\boldsymbol{T_{sto-y}}$	Satellite's vehicle storage time (y-direction)
$\boldsymbol{T_{rel}}$	Relocation time of a dual command cycle
$\boldsymbol{T_{rel-load}}$	Satellite's vehicle time for loading the blocking SKU (y-direction)
$\boldsymbol{T_{rel-unload}}$	Satellite's vehicle time for unloading the blocking SKU (y-direction)
$\boldsymbol{T_{rel-x}}$	Shuttle's carrier relocation time (x-direction)
$\boldsymbol{T_{ret}}$	Retrieval operation time of a dual command cycle
$\boldsymbol{T_{ret-x}}$	Shuttle's carrier retrieval time (x-direction)
$\boldsymbol{T_{ret-y}}$	Satellite's vehicle retrieval time (y-direction)
$\boldsymbol{v}$	Velocity
$\boldsymbol{v_x}$	Maximum velocity of a shuttle carrier alongside columns (x-direction)

v_y	Maximum velocity of a satellite vehicle in depth (y-direction)
w_0	Width of a corridor (y-direction)
w_{SKU}	Width of an SKU
w_{ss}	Width of a storage location in-depth (y-direction)
W	SKU configuration matrix of the AVS/RS

3.2 Dual command cycle

Shuttle carrier can perform either a Single Command (SC) or a Dual Command (DC) cycle. An SC cycle can be performed for both the storage or retrieval process. In contrast, the DC cycle is always a combination of storage and a retrieval process. Compared to an SC, a DC is more efficient, as the shuttle carrier performs less ineffective empty travel operation relative to the handled SKUs.

The DC cycle (Figure 2) begins by loading the SKU from the buffer location to the shuttle carrier and travelling to the selected storage location. The storing process then continues with the unloading of SKU in a specific depth of the storage rack by utilising a satellite vehicle. Once the satellite vehicle returns to the shuttle carrier, the shuttle carrier begins the retrieval process by travelling (empty) to the retrieval location where an ordered (retrieving) SKU is stored. This paper studies an undetermined retrieval sequence problem, meaning that a uniform random function selects retrieval sequence among all SKUs in AVS/RS. If the ordered (retrieving) SKU is blocked by one or more blocking SKUs, a relocation cycle begins, where all blocking SKUs have to be relocated to another empty storage location.

The satellite vehicle first loads a blocking SKU to the shuttle carrier. Then the shuttle carrier travels to an empty storage location, selected by a relocation assignment strategy. The blocking SKU is unloaded to the designated empty storage location. Next, the shuttle carrier returns to the retrieving SKU location, and the relocation cycle repeats if there is another SKU blocking the ordered (retrieving) SKU.

When all of the blocking SKUs have been relocated, the shuttle carrier loads the ordered (retrieving) SKU by utilising the satellite vehicle. Finally, the shuttle carrier returns to the buffer location where SKU is unloaded to the buffer position, and the DC cycle completes.

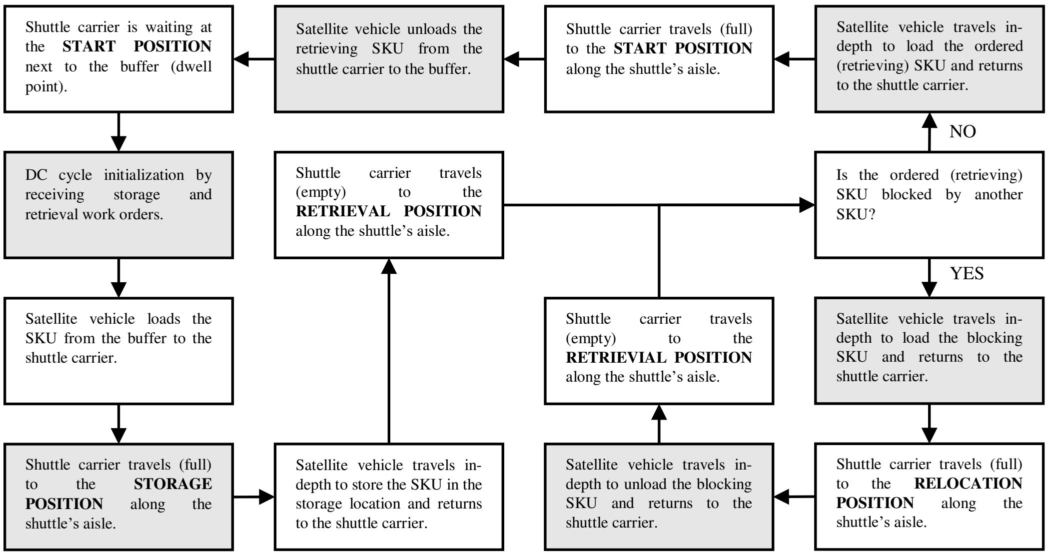

Figure 2: Process flow diagram for the DC cycle

The DC cycle time is calculated by summing individual times for the above-mentioned DC processes and equals Equation (1):

$$T_{DCC} = T_{sto} + T_{ret} + T_{et} + \omega_{rel} T_{rel} \tag{1}$$

The DC cycle time is associated with the shuttle carrier and satellite vehicle travelling in the horizontal (x) and (y) directions, respectively. Equation (1) can be further extended with the following expression Equation (2):

$$T_{DCC} = 2 \cdot T_{buf} + T_{sto-x} + T_{sto-y} + T_{ret-x} + T_{ret-y} + T_{et} + \omega_{rel}(T_{rel-load} + 2T_{rel-x} + T_{rel-unload}) \tag{2}$$

The DC cycle time is affected by selecting the appropriate storage and relocation strategy. The storage strategy directly impacts the average storage time of the shuttle's vehicle in the horizontal (x) direction T_{sto-x} and satellite vehicle in horizontal (y) direction T_{sto-y}. Likewise, the relocation strategy directly impacts the average number of relocations ω_{rel}, the average loading time of the blocking SKU to the shuttle carrier $T_{rel-load}$, average shuttle's carrier relocation travel time in the horizontal (x) direction T_{rel-x} and average unloading time of the blocking SKU $T_{rel-unload}$. However, both storage and relocation strategy indirectly impact the average empty travel T_{et}, average shuttle's carrier retrieval time T_{ret-x} and average satellite vehicles retrieval time of the ordered (retrieving) SKU T_{ret-y}.

3.3 Kinematic model of the shuttle carrier and the satellite vehicle

A widely used kinematic model has been applied to describe the shuttle carrier's and satellite vehicle's kinematic performance in similar research studies [4], [6], [7], [15], [18], [22], [23]. The kinematic model determines the amount of time the vehicle needs for travelling a certain distance based on maximum velocity, acceleration, and deceleration.

The model approximates the vehicle velocity function by a constant acceleration and deceleration. When the vehicle reaches its maximum velocity, the acceleration stops, and the vehicle travels with a constant velocity. If the acceleration and the deceleration are not of the same value, a parameter (a) can be determined by Equation 3:

$$a = \frac{2a_1 a_2}{a_1 + a_2} \tag{3}$$

The vehicle reaches its maximum velocity after it travels a sufficient distance $(s_{critical})$ Equation 4:

$$s_{critical} = \frac{v^2}{a} \tag{4}$$

If the travel distance (s) is shorter than the critical distance $(s_{critical})$, the vehicle never reaches its maximum velocity and starts to decelerate exactly when half of the distance has been travelled. If the travel distance is longer than the critical distance, the vehicle reaches its maximum velocity. When these two notions are merged, Equation 5 is obtained:

$$t(s) = \begin{cases} 2\sqrt{\frac{s}{a}}, & if\ s < \frac{v^2}{a} \\ \frac{s}{v} + \frac{v}{a}, & otherwise \end{cases} \tag{5}$$

3.4 Column and depth time calculation

Shuttle carrier travels along the aisle in the horizontal (x) direction, while for accessing storage location in-depth in horizontal (y) direction, a satellite vehicle is utilised. In our simulation model, both vehicles follow the same kinematic model described in Section 3.3.

The satellite vehicle must travel in-depth for accessing SKUs in the buffer or any arbitrary depth of the storage rack. The corresponding times of satellite vehicle operations are (T_{buf}) for accessing SKUs in the buffer, (T_{sto-y}) for storing SKUs, (T_{ret-y}) for retrieving SKUs, ($T_{rel-load}$) for loading the blocking SKUs and finally ($T_{rel-unload}$) for unloading the blocking SKU.

The satellite vehicle operations always consist of travelling in-depth ($t_{in/out}$), loading or unloading the SKU and travelling back to the shuttle carrier ($t_{in/out}$), Equation (6):

$$t_{depth} = 2t_{in/out} + t_{load/unload} \tag{6}$$

The satellite vehicle always travels from the shuttle carrier towards the designated depth (d_d). Because the corridor width (w_0) is usually a bit wider than the width of a storage location (w_{ss}), the one-way path distance of a satellite vehicle can be calculated by Equation (7):

$$s(d_d) = \frac{w_0 + w_{ss}}{2} + (d_d - 1) \cdot w_{ss} \tag{7}$$

Satellite vehicle travel time can be calculated by Equation (8):

$$t_{depth}(d_d) = t_{load/unload} + 2 \cdot \begin{cases} 2\sqrt{\dfrac{\frac{w_0 + w_{ss}}{2} + (d_d - 1) \cdot w_{ss}}{a_y}}, & if\ \dfrac{w_0 + w_{ss}}{2} + (d_d - 1) \cdot w_{ss} < \dfrac{v_y^2}{a_y} \\ \dfrac{\frac{w_0 + w_{ss}}{2} + (d_d - 1) \cdot w_{ss}}{v_y} + \dfrac{v_y}{a_y}, & otherwise \end{cases} \quad (8)$$

The shuttle carrier conveys SKUs and satellite vehicle along the AVS/RS aisle in (x) direction. It carries out storage operations in time (T_{sto-x}), retrieval operations in time (T_{ret-x}), empty travel operations in time (T_{et}) and relocation operations in time (T_{rel-x}). Opposite to the satellite vehicle, trips are always performed only in one direction, and there is no loading nor unloading time requirement. When the shuttle carrier performs a storage or retrieval operation, the path distance equation has to include the extra length from the buffer to the first storage location (l_0), designated column (c_d) and storage slot length (l_{ss}), Equation (9):

$$s(c_d) = l_0 + (c_d - 1) \cdot l_{ss} \quad (9)$$

The shuttle carrier travel time equation for storage or retrieval operation can be calculated by Equation (10):

$$t_{column}(c_d) = \begin{cases} 2\sqrt{\dfrac{l_0 + (c_d - 1) \cdot l}{a_x}}, & if\ l_0 + (c_d - 1) \cdot l < \dfrac{v_x^2}{a_x} \\ \dfrac{l_0 + (c_d - 1) \cdot l}{v_x} + \dfrac{v_x}{a_x}, & otherwise \end{cases} \quad (10)$$

Shuttle carriers' empty travel and relocation operations always occur along the shuttle carriers' aisle (never includes the buffer location). Therefore, the distance equation is dependant only on the storage slot length (l_{ss}), starting column (c_s) and designated column (c_d), Equation (11):

$$s(c_s, c_d) = |c_d - c_s| \cdot l_{ss} \quad (11)$$

Lastly, the shuttle carrier's travel time for an empty travel and a relocation operation can be calculated by Equation (12):

$$t_{column}(c_s, c_d) = \begin{cases} 2\sqrt{\dfrac{|c_d - c_s| \cdot l_{ss}}{a_x}}, & if\ |c_d - c_s| \cdot l_{ss} < \dfrac{v_x^2}{a_x} \\ \dfrac{|c_d - c_s| \cdot l_{ss}}{v_x} + \dfrac{v_x}{a_x}, & otherwise \end{cases} \tag{12}$$

3.5 Storage and relocation assignment strategies

Whenever an arriving SKU needs to be stored, a storage location has to be selected via the storage strategy. Likewise, a storage location has to be selected during the relocation cycle whenever another SKU blocks an ordered (retrieving) SKU. Both storage and relocation strategies have a significant impact on the AVS/RS performance. The objective of storage and relocation strategies is a selection of the appropriate empty location by accomplishing two goals. First, to minimise the current command cycle's travel time and second, reduce future command cycles' travel time.

For selecting a suitable empty storage location, the current shuttle carrier position ($c_{shuttle}$), the SKUs configuration in AVS/RS (W), the side (location) of the ordered (retrieving) SKU (s_{SKU}) and the corresponding strategy has to be known. During the storage process, the shuttle carrier starting position is always at the buffer. In contrast, during the relocation cycle, the shuttle carrier position varies, depending on the ordered (retrieving) SKU location. That is why the storage and relocation strategies can have the same form and can be therefore expressed with the same function.

In continuation, three different storage and relocation assignment strategies are presented. These are already well known (i) random strategy and (ii) nearest neighbour strategy along with our proposed strategy called (iii) depth-first. Consequently, there are in total of nine (9) different combinations of storage and relocation assignment strategies.

Random strategy

Random strategy (RAND) selects an empty storage location by using a random function. Many articles have studied a random strategy, especially during the storage process [4], [6], [7], [15], [18], [22], [23]. However, the selection is not always entirely random, as all empty storage locations are usually not considered. The selection of a storage or relocation location is made only from the most in-depth empty storage locations to prevent empty storage locations in between two occupied storage locations.

Nearest neighbour strategy

The second strategy, also applied by other researchers, is the nearest neighbour (NN) strategy [4], [6], [7], [21], [22]. The SKU is stored or relocated to the nearest available empty location (Figure 3 – left). If possible, the nearest storage location is often the one on the opposite side of the retrieving SKU. Otherwise, gradually further from the shuttle carrier location. If there is more than one empty location available in the selected nearest rack lane, the heuristic rule chooses the deepest one. In general, the NN strategy primarily minimises a shuttle carrier's travelled distance and secondarily maximises the satellite vehicle's depth travel distance.

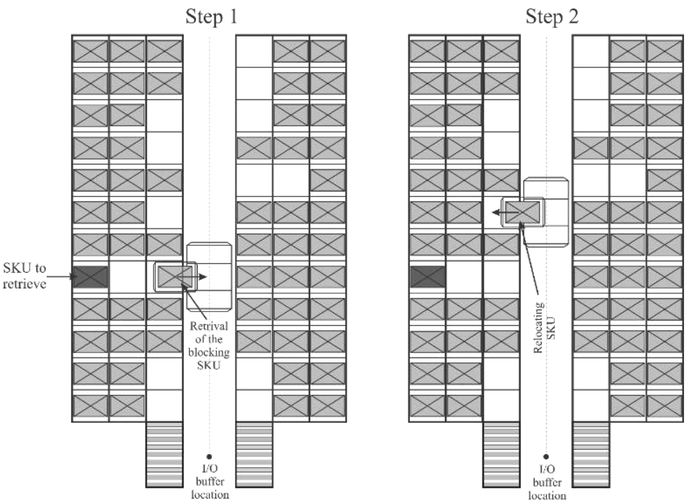

$\boldsymbol{Input}: W, c_{shuttle}, s_{SKU}$
$s = \frac{2 \cdot s_{SKU}}{s_{SKU}^2}$
$\boldsymbol{for}\ d = D\ to\ 1\ \boldsymbol{do}$
$\quad \boldsymbol{if}\ W(d, c_{shuttle}, s) = 0\ \boldsymbol{then}$
$\quad\quad \boldsymbol{output} = [d, c_{shuttle}, s]$
$\quad\quad \boldsymbol{exit}$
$\boldsymbol{for}\ c = 1\ to\ (C-1)$
$\quad \boldsymbol{for}\ d = D\ to\ 1\ (step = -1)$
$\quad\quad \boldsymbol{for}\ s = 1\ to\ 2$
$\quad\quad\quad \boldsymbol{if}\ c_{shuttle} + c \leq C\ \boldsymbol{then}$
$\quad\quad\quad\quad \boldsymbol{if}\ W(d, c_{shuttle} + c, s) = 0\ \boldsymbol{then}$
$\quad\quad\quad\quad\quad \boldsymbol{output} = [d, c_{shuttle} + c, s]$
$\quad\quad\quad\quad\quad \boldsymbol{exit}$
$\quad\quad\quad \boldsymbol{if}\ c_{shuttle} - c \geq 1\ \boldsymbol{then}$
$\quad\quad\quad\quad \boldsymbol{if}\ W(d, c_{shuttle} - c, s) = 0\ \boldsymbol{then}$
$\quad\quad\quad\quad\quad \boldsymbol{output} = [d, c_{shuttle} - c, s]$
$\quad\quad\quad\quad\quad \boldsymbol{exit}$

Figure 3: Nearest neighbour relocation assignment strategy example (left) and pseudo-code algorithm (right)

In Figure 3 – right, a pseudo-code for the NN strategy is given. The algorithm starts with the initialisation of the current shuttle carrier position ($c_{shuttle}$), the SKU configuration in AVS/RS (W) and the side (location) of the ordered (retrieving) SKU (s_{SKU}). The first 'for loop' (lines 3-6) gradually checks for an empty location at the other side of the ordered (retrieving) SKU. If the empty location is found (line 4), the algorithms output the selected empty location coordinates and exits. If the condition has not been met, the algorithm continues with the next 'for loop' (lines 7-17). The second loop gradually tests for the emptiness of storage locations further from the shuttle's vehicle current position ($c_{shuttle}$), by increasing the column index (c). The depth index (d) for empty storage location starts at the deepest possible depth (D) and incrementally (with step -1) decreases to 1. Each position with column index (c) and depth index (d) is tested for empty storage location, first at one side and second at the other. Once the empty storage location has been found, the algorithm outputs its coordinates and exits.

Depth-first strategy

The third strategy considered is the depth-first (DF) strategy. In this case, the storing or blocking SKU is relocated to the most in-depth possible empty storage location (Figure 4 – left). If there are more than one empty storage locations at the most in-depth level, the blocking SKU is relocated to the storage location closest to the shuttle carrier's position. The DF strategy is sometimes applied in container terminals, where a similar relocation problem emerges whenever another container blocks the ordered (retrieving) one. Opposite to the NN strategy, the DF strategy primarily maximises satellite vehicle travel distance and secondarily minimises the shuttle carrier travel distance.

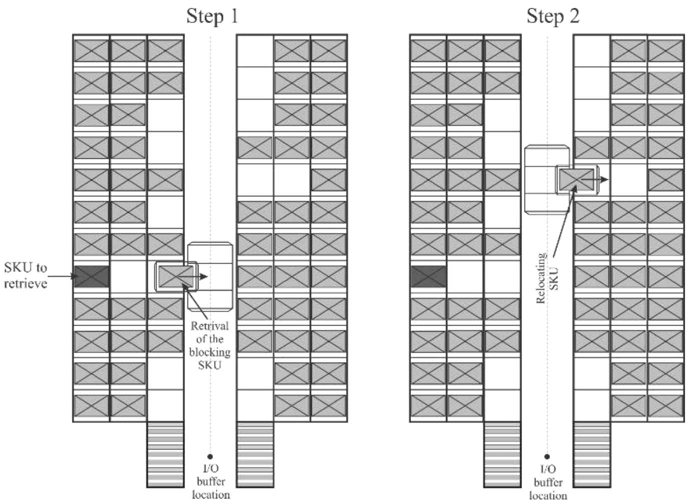

1. $\boldsymbol{Input}: W, c_{shuttle}, s_{SKU}$
2. $\boldsymbol{for}\ d = D\ to\ 1\ (step = -1)\ \boldsymbol{do}$
3. $\quad s = \frac{2 \cdot s_{SKU}}{s_{SKU}^2}$
4. $\quad \boldsymbol{if}\ W(d, c_{shuttle}, s) = 0\ \boldsymbol{then}$
5. $\quad\quad \boldsymbol{output} = [d, c_{shuttle} - c, s]$
6. $\quad\quad \boldsymbol{exit}$
7. $\quad \boldsymbol{else}$
8. $\quad\quad \boldsymbol{for}\ c = 1\ to\ (C - 1)$
9. $\quad\quad\quad \boldsymbol{for}\ s = 1\ to\ 2$
10. $\quad\quad\quad\quad \boldsymbol{if}\ c_{shuttle} + c \leq C\ \boldsymbol{then}$
11. $\quad\quad\quad\quad\quad \boldsymbol{if}\ W(d, c_{shuttle} + c, s) = 0\ \boldsymbol{then}$
12. $\quad\quad\quad\quad\quad\quad \boldsymbol{output} = [d, c_{shuttle} + c, s]$
13. $\quad\quad\quad\quad\quad\quad \boldsymbol{exit}$
14. $\quad\quad\quad\quad \boldsymbol{if}\ c_{shuttle} - c \geq 1\ \boldsymbol{then}$
15. $\quad\quad\quad\quad\quad \boldsymbol{if}\ W(d, c_{shuttle} - c, s) = 0\ \boldsymbol{then}$
16. $\quad\quad\quad\quad\quad\quad \boldsymbol{output} = [d, c_{shuttle} - c, s]$
17. $\quad\quad\quad\quad\quad\quad \boldsymbol{exit}$

Figure 4: Depth-first relocation assignment strategy example (left) and pseudo-code algorithm (right)

In Figure 4 – right, a pseudo-code for the DF strategy is given. The algorithm starts with the initialisation of the current shuttle carrier position ($c_{shuttle}$), the SKU configuration in AVS/RS (W) and the side (location) of the ordered (retrieving) SKU (s_{SKU}). There is a single main 'for loop' (lines 2-17) that gradually decreases depth index (d) from (D) to 1. At each depth index (d) the algorithm check for an empty storage location. First, on the opposite side of the ordered (retrieving) SKU (s_{SKU}) and then gradually away from the current shuttle carrier position ($c_{shuttle}$) (at both sides of the aisle). Once that the empty storage location has been found, the algorithm outputs its coordinates and exits.

3.6 Space area utilisation and fill-grade factor

Fill-grade factor

Fill-grade factor (α), also known as filling degree, is a widely used parameter by other authors in related work [4], [7], [22]. It defines the occupancy level of the AVS/RS and can be calculated by dividing the number of occupied storage locations (N_{os}) with the number of all storage locations (N) (occupied and empty) in the AVS/RS, Equation (13):

$$\alpha = \frac{N_{os}}{N} = \frac{N_{os}}{N_{os} + N_{es}} \tag{13}$$

Space area utilisation

Multi-deep AVS/RS has better space area utilisation (η_{area}) compared to a single-deep AVS/RS. The space area utilisation (η_{area}) can be calculated by comparing (useful) area intended for storage ($A_{storage}$) to the entire area of AVS/RS that is composed of a storage area ($A_{storage}$) and shuttle carrier's aisle area (A_{aisle}), Equation (16).

$$\eta_{area} = \frac{A_{storage}}{A_{storage} + A_{aisle}} \tag{16}$$

Space area utilisation (η_{area}) is independent of the number of columns (C) or the length of a storage location (l_{ss}), as the width of the AVS/RS shuttle carrier's aisle does not change in horizontal (x) direction. The only key parameters are the number of depths (D), the width of the shuttle carrier's aisle (w_0) and the width of a storage location (w_{ss}), Equation (17).

$$\eta_{area} = \frac{Dw_{ss}}{Dw_{ss} + w_0} \tag{17}$$

4 Results

4.1 Input data

Our research study was based on the simulation model developed in MATLAB R2020b Simulink software. The main toolboxes used were Simevents and Stateflow. The simulation model ran on a standard PC with an Intel i9 @3.6 GHz processor and 64 GB of RAM. Simulation input data is provided in the following paragraph.

The storage location dimensions were based on the dimensions of an SKU with a length $l_{SKU} = 0.4\ m$ and width $w_{SKU} = 0.6\ m$. The height of the SKU was irrelevant in this case as the simulation model only focused on a single level of AVS/RS. The distance between two consecutive storage locations along the aisle was set to $l_{ss} = 0.5\ m$ and in-depth to $w_{ss} = 0.7\ m$. The distance between the buffer (I/O point) and the first storage location was set to $l_0 = 1.5\ m$. The width of an aisle for operating a shuttle carrier was set to $w_0 = 1\ m$.

Dimensions of the AVS/RS storage rack varies from the number of columns C in the horizontal (x) direction and the number of depths D in the horizontal (y) direction. In total, five (5) different AVS/RS configurations were studied in this paper. All studied AVS/RS configurations have 1200 storage locations (600 on each side of the storage aisle). Additionally, every AVS/RS case study was considered with ten (10) different occupancy levels by varying fill grade factor (α). AVS/RS configuration input parameters are given in Table 2.

The shuttle carrier and the satellite vehicle were modelled based on the kinematic model (Section 3.3 and 3.4). The simulation model corresponds to the acceleration and maximum velocity parameters of the shuttle carrier and the satellite vehicle. As the satellite vehicle also performs the loading and unloading of SKUs, additional parameter ($t_{load/unload}$) has to be provided. The shuttle carrier's and satellite vehicle's kinematic parameters are also provided in Table 2.

Table 2: Shuttle carrier's and satellite vehicle's kinematic parameters

Parameter	**Symbol**	**Input parameter value**
Number of columns	C	$\{100, 120, 150, 200, 300\}$
Number of depths	D	$\{6, 5, 4, 3, 2\}$
Fill factor-alpha	α	$\{55\%, 60\%, 65\%, 70\%, 75\%, 80\%, 85\%, 90\%, 95\%\}$
Shuttle carrier acceleration	a_x	$2\ m/s^2$
Shuttle carrier (max.) velocity	v_x	$3\ m/s$
Satellite vehicle acceleration	a_y	$1\ m/s^2$
Satellite vehicle (max.) velocity	v_y	$1.5\ m/s$
Loading and unloading time	$t_{load/unload}$	$1\ s$

Note: Loading and unloading of SKU is performed by the lifting mechanism on the satellite vehicle, for which the loading and unloading times are relatively short. Usually, in real applications, the fill grade factor $\alpha > 85\%$.

4.2 Case study results

In this section, the results of a case study are presented for five (5) AVS/RS configurations, with nine (9) different combinations of storage and relocation assignment strategies. Dual command cycle times (DC) are provided as a mean value of all DC cycles performed during a $T = 3 \cdot 10^6\ sec$ simulation time. Our research aims to find the best combination of storage and relocation assignment strategy, which would give us the highest throughput performance $\lambda(DC)$ and, consequently, the shortest mean DC cycle time. The numerical simulation results for every AVS/RS configuration are presented in Table 5 (Appendix).

Double-deep AVS/RS

Figure 5 shows the results for a double-deep AVS/RS ($D = 2$) with 300 columns ($C = 300$). The combination of the 'NN storage and NN relocation' assignment strategy gives us the best results for the mean DC cycle time under the fill-grade factor ($\alpha \leq 85\%$). Meanwhile, the

'RAND storage and RAND relocation' assignment strategies combination performed with the highest DC cycle time, independent of the fill-grade factor (α). Based on the fill-grade factor, one can notice that at 90% occupancy ($\alpha = 90\%$), the combination of the 'DF storage and NN relocation' assignment strategy performed with the highest throughput performance. However, at an occupancy level of 95% ($\alpha = 95\%$), the 'RAND storage and NN relocation' assignment strategy outperformed all other strategies combinations.

All storage and relocation assignment strategies combination display an approximate linear dependency to the increasing fill-grade factor (α), except for a 'DF storage and NN relocation' and a 'DF storage and DF relocation' assignment strategies combination. These two strategies combinations resulting mean DC cycle times are in a concave shape and are overlapping one another independent of fill grade factor (α). This is because, in a double-deep AVS/RS, the 'DF storage' assignment strategy will always fill with priority the storage location at a second depth (if during a retrieval cycle, SKU was taken from the second depth). With all of the storage locations occupied at a second depth, the 'DF relocation' assignment strategy performs exactly the same as the 'NN relocation' assignment strategy, i.e., minimising the shuttle carrier's travel distance.

The lowest differences of the mean DC cycle time correspond to the 'NN storage and RAND relocation' assignment strategies combination, independent of the fil-grade factor (α). Strategies combinations with such attributes are useful for developing analytical travel time models since the dependencies are not complex and can be calculated with high accuracy.

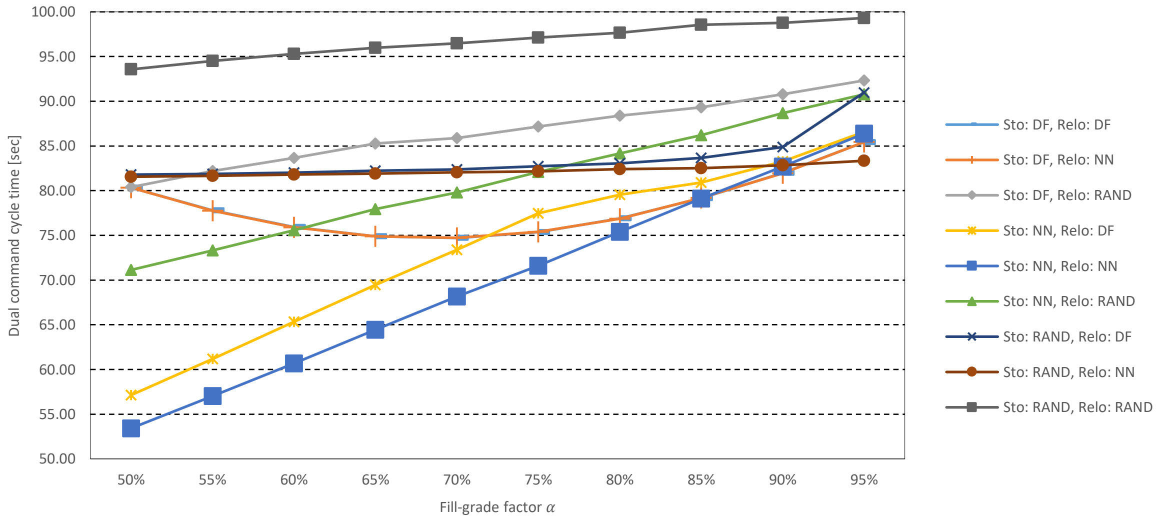

Figure 5: DC cycle time of a double-deep AVS/RS ($D = 2$ and $C = 300$)

Triple-deep AVS/RS

In Figure 6, the simulation results for a triple-deep AVS/RS ($D = 3$) with 200 columns ($C = 200$) are presented. At a low fill-grade factor ($\alpha \leq 60\%$), the 'NN storage and NN relocation' assignment strategies combination performed with the lowest mean DC cycle time. At a higher fill-grade factor ($\alpha > 60\%$), the 'DF storage and NN relocation' outperform the 'NN storage and NN relocation' assignment strategies combination.

Unlike the 'DF storage and DF relocation' assignment strategies combination, all of the presented strategies combinations display a growing tendency in the relationship of the increasing fill-grade factor (α). As the AVS/RS gets more occupied, the number of empty storage locations gets smaller, meaning that the shuttle carrier has to travel longer travel distances for both storage and relocation operations. In Figure 10, one assignment strategies combination ('DF storage and DF relocation') shows different mean DC travel time dependencies than other assignment strategies. It happens that after the fill-grade factor (α) exceeds 70% ($\alpha > 70\%$), the mean DC cycle time begins to decrease. The explanation for such behaviour is the characteristic of the 'DF storage and DF relocation' assignment strategies combination to fulfil the most in-depth storage locations first. At approx. 67% occupancy ($\alpha \approx 67\%$) in a triple deep AVS/RS, the third and the second depth are entirely filled. In such cases, there are large distances between the location of retrieving SKU and relocation storage locations because there are few empty storage locations at maximum depth. As the occupancy level increases above 70%, the number of empty storage locations begins to grow. Consequently, the travel distance between retrieving SKU and relocation storage location begins to decline. At fill-grade factor ($\alpha = 85\%$), the path distances between neighbourly empty storage locations are the shortest. The mean DC cycle time of the 'DF storage and DF relocation' assignment strategies combination reaches a local minimum. Larger fill-grade factors ($\alpha > 85\%$) cause the expected increase of DC cycle times.

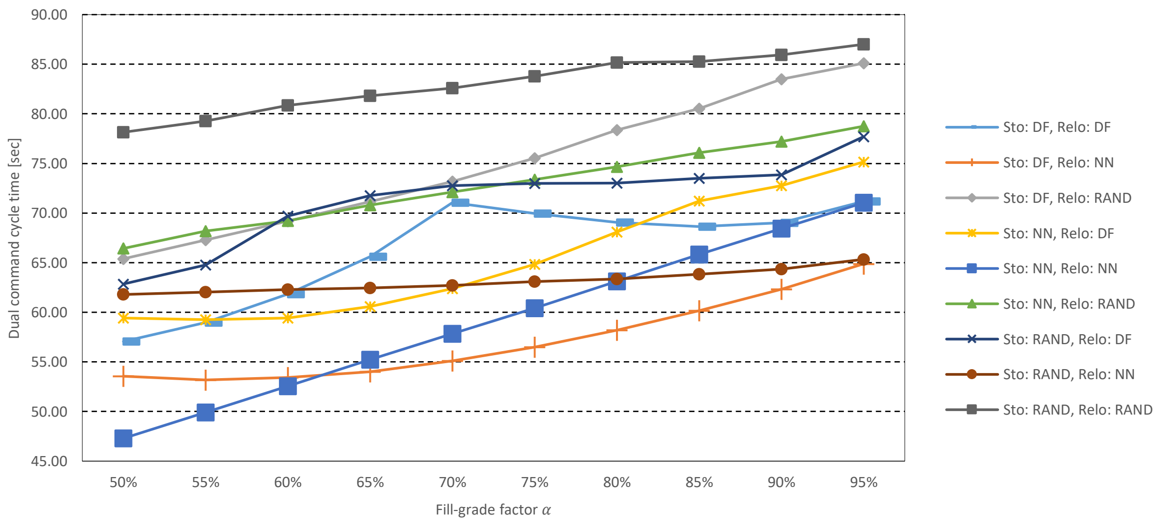

Figure 6: DC cycle time of a triple-deep AVS/RS ($D = 3$ and $C = 200$)

Fourfold-deep AVS/RS

The simulation results for a fourfold-deep AVS/RS ($D = 4$) with 150 columns ($C = 150$) are presented in Figure 7. The best performing assignment strategies combination, when fill-grade factor ($\alpha \leq 90\%$), was 'DF storage and NN relocation'. At the highest simulated occupancy ($\alpha = 95\%$), the shortest DC cycle time was achieved with the 'RAND storage and NN relocation' assignment strategies combination. The 'RAND storage and RAND relocation' again performed with the longest mean DC cycle time.

'DF storage and DF relocation' assignment strategies combination have a similar pattern as in a case study configuration with triple-deep AVS/RS and 200 columns ($D = 3$ and $C = 200$). However, in a fourfold-deep AVS/RS case, the third depth gets filled at fill-grade factor ($\alpha = 75\%$). Shorter mean DC cycle times at fill-grade factor ($\alpha > 75\%$) can be explained with the same concept as in a case study with a triple-deep AVS/RS.

According to the relocation assignment strategy, one can notice that the best solutions (lowest mean DC cycle time) are achieved by using the 'NN relocation' assignment strategy. Meanwhile, the longest mean DC cycle times are always performed by using the 'RAND relocation' assignment strategy.

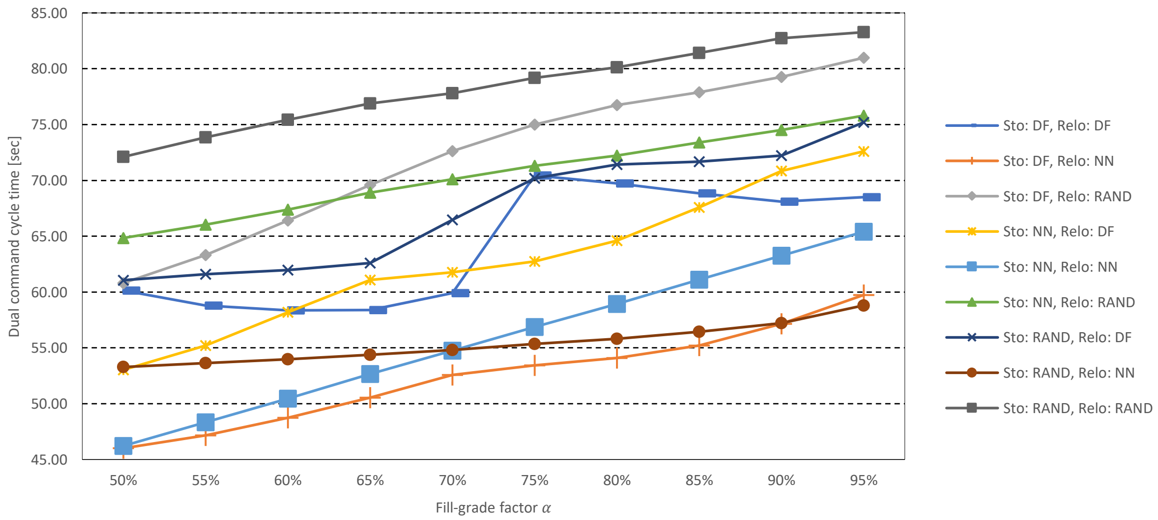

Figure 7: DC cycle time result of a fourfold-deep AVS/RS ($D = 4$ and $C = 150$)

Fivefold-deep AVS/RS

In Figure 8, the simulation results for a fivefold-deep AVS/RS ($D = 5$) with 120 columns ($C = 120$) are shown. Independent of the fill-grade factor (α), the shortest mean DC cycle time was accomplished with a 'DF storage and NN relocation' assignment strategies combination.

'DF storage and DF relocation' assignment strategies combination show a distinct 'zigzag' pattern, as the third depth get filled at fill-grade factor ($\alpha = 60\%$), and the fourth depth gets filled at fill-grade factor ($\alpha = 80\%$). Note, the explanation of this relationship is already explained in the case of a triple-deep AVS/RS.

The storage and relocation assignment strategies combinations can be again categorised into three groups based on the applied relocation assignment strategy. The first group (I. – see Figure 8) of strategies combinations that include the 'RAND relocation' assignment strategy achieve the longest mean DC cycle times. The next group (II. – see Figure 8) consists of the three strategies combinations that all use the 'DF relocation' assignment strategy and completed moderate mean DC cycle times. The shortest mean DC cycle times are achieved by the last group (III. – see Figure 8) of assignment strategies combinations that include the 'NN relocation' assignment strategy.

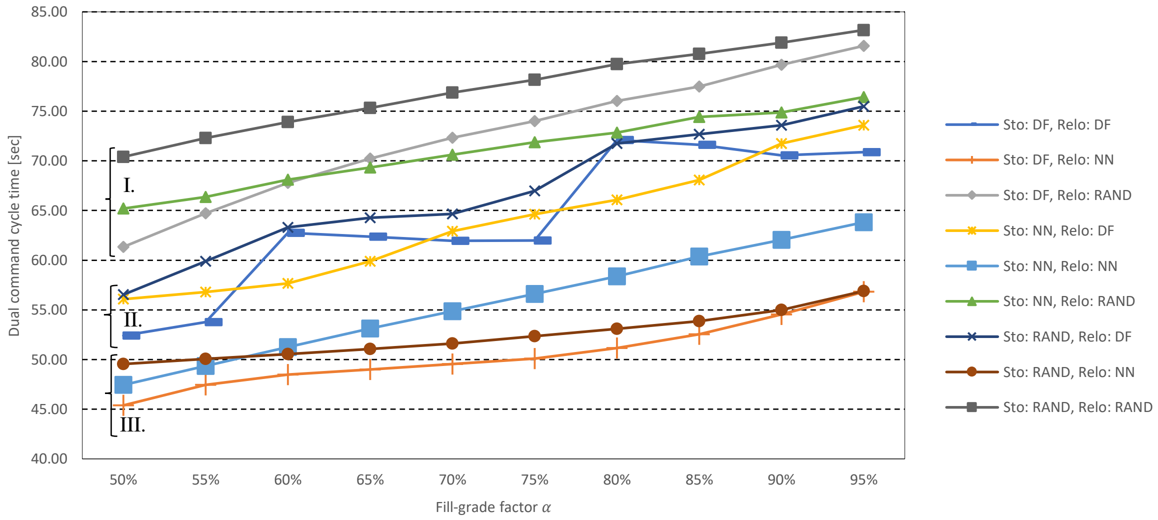

Figure 8: DC cycle time result of a fivefold-deep AVS/RS ($D = 5$ and $C = 120$)

Sixfold-deep AVS/RS

Lastly, in Figure 9, the simulation results of a sixfold-deep AVS/RS ($D = 6$) with 100 columns ($C = 100$) are presented. Likewise to the case of a fivefold-deep AVS/RS, the shortest mean DC cycle time was accomplished with 'DF storage and NN relocation' assignment strategies combination (independent of fill-grade factor (α)).

The 'DF storage and DF relocation' assignment strategies combination yet again display a 'zigzag' pattern. The reasoning behind the pattern was already explained in a triple-deep AVS/RS case. The local maximums appear whenever a depth gets filled ($\alpha = 50\%$, $\alpha = 66.7\%$ and $\alpha = 83.3\%$).

The simulation results show that the relocation assignment strategy majorly impacts the DC cycle times, as the storage and relocation assignment strategies combinations can be again grouped into three groups according to the utilised relocation strategy. The first three storage and relocation assignment strategies combinations with the shortest mean DC cycle times all use the 'NN relocation' assignment strategy. The next three utilise the 'DF relocation' assignment strategy and the last three the 'RAND assignment' strategy.

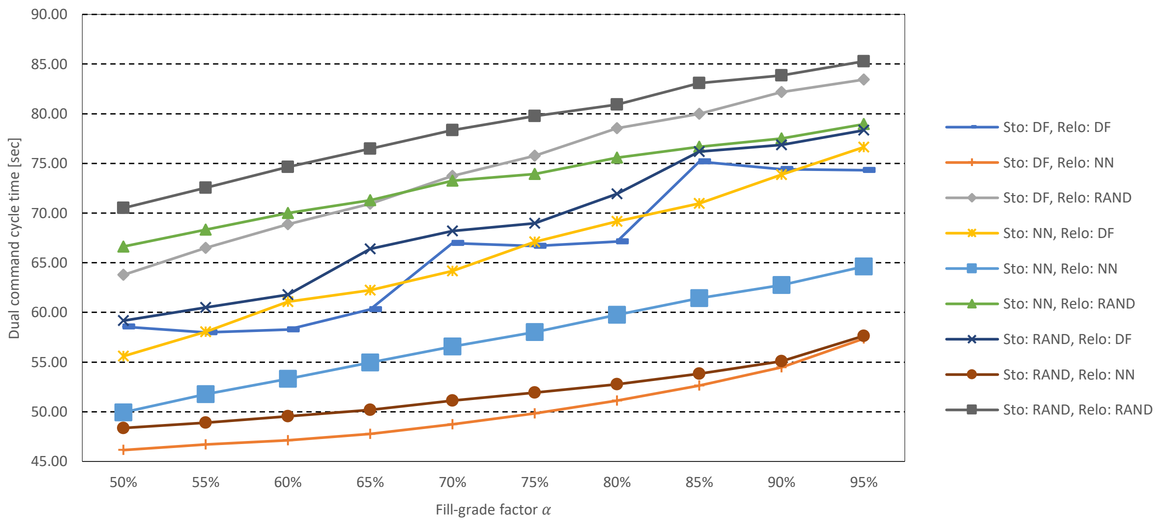

Figure 9: DC cycle time result of a sixfold-deep AVS/RS ($D = 6$ and $C = 100$)

Summary

Overall, by increasing the fill-grade factor (α), most strategies combinations show a moderate growth of mean DC cycle times, resulting in a lower AVS/RS throughput performance.

The shortest mean DC cycle times at different fill-grade factors (α) are summarised in Table 3. It appears that fivefold and sixfold-deep AVS/RS with the 'DF storage and NN relocation' assignment strategies combination outperforms the other strategies combinations and AVS/RS storage rack configurations. Furthermore, sixfold-deep AVS/RS have the highest space area utilisation (η_{area}) as the ratio between the storage area and the shuttle carrier's aisle area is the highest.

Table 3: Summary of simulation results with the shortest DC cycle times at various fill-grade factors (α)

Fill-grade factor (α)	C	D	$T(DC)$ **[sec/cycle]**	**Storage assignment strategy**	**Relocation assignment strategy**	$\lambda(DC)$ **[tote/ hour]**	η_{area} [%]
α = 50%	120	5	45.38	DF	NN	158.64	77.78
α = 55%	100	6	46.70	DF	NN	154.16	80.77
α = 60%	100	6	47.12	DF	NN	152.80	80.77
α = 65%	100	6	47.76	DF	NN	150.74	80.77
α = 70%	100	6	48.73	DF	NN	147.76	80.77
α = 75%	100	6	49.82	DF	NN	144.52	80.77
α = 80%	100	6	51.11	DF	NN	140.88	80.77
α = 85%	120	5	52.54	DF	NN	137.04	77.78
α = 90%	100	6	54.46	DF	NN	132.22	80.77
α = 95%	120	5	56.82	DF	NN	126.72	77.78

Note: The throughput performance of AVS/RS was calculated by $\lambda(DC) = 2\frac{3600}{T(DC)}$.

The 'DF storage and NN relocation' assignment strategies combination achieved the shortest mean DC cycle times in most study cases, especially in deeper AVS/RS. The 'DF storage' assignment strategy ensures that the deepest storage locations are filled first. Because selecting the ordered (retrieving) SKUs was random, the 'DF storage' strategy also provided an even distribution between neighbourly empty storage locations. On the other hand, the 'NN relocation' assignment strategy ensured a quick relocation process, as the travel distance between retrieval SKU and relocation position was the shortest.

4.3 Storage and relocation assignment strategies benchmark

In continuation, nine (9) storage and relocation assignment strategies combination are benchmarked for three (3) different fill-grade factor (α) (Table 4): low occupancy ($\alpha = 60\%$), medium occupancy ($\alpha = 75\%$) and high occupancy ($\alpha = 90\%$).

Table 4: Storage and relocation assignment strategies combination benchmark at a low, medium and high occupancy level of AVS/RS

	Storage strategy	Relocation strategy	$D = 2, C = 300$	$D = 3, C = 200$	$D = 4, C = 150$	$D = 5, C = 120$	$D = 6, C = 100$
Fill-grade factor $\alpha = 60$ %	DF	DF	25.15%	17.67%	19.71%	29.43%	23.64%
	DF	NN	25.13%	1.64%	**0.00%**	**0.00%**	**0.00%**
	DF	RAND	37.91%	31.65%	36.24%	39.76%	46.16%
	NN	DF	7.68%	13.06%	19.33%	18.89%	29.62%
	NN	NN	**0.00%**	**0.00%**	3.50%	5.66%	13.10%
	NN	RAND	24.55%	31.68%	38.24%	40.47%	48.55%
	RAND	DF	35.22%	32.59%	27.12%	30.51%	31.09%
	RAND	NN	34.83%	18.49%	10.74%	4.23%	5.12%
	RAND	RAND	57.07%	53.81%	54.73%	52.43%	58.44%
Fill-grade factor $\alpha = 75$ %	DF	DF	5.21%	23.86%	31.86%	23.74%	33.87%
	DF	NN	5.30%	**0.00%**	**0.00%**	**0.00%**	**0.00%**
	DF	RAND	21.71%	33.69%	40.41%	47.71%	52.09%
	NN	DF	8.20%	14.76%	17.44%	29.01%	34.68%
	NN	NN	**0.00%**	6.95%	6.46%	13.01%	16.44%
	NN	RAND	14.64%	29.88%	33.48%	43.49%	48.42%
	RAND	DF	15.51%	29.19%	31.41%	33.66%	38.47%
	RAND	NN	14.73%	11.67%	3.62%	4.50%	4.20%
	RAND	RAND	35.60%	48.31%	48.23%	56.04%	60.12%
Fill-grade factor $\alpha = 90$ %	DF	DF	2.50%	9.71%	16.51%	24.72%	29.56%
	DF	NN	2.51%	**0.00%**	1.59%	**0.00%**	**0.00%**
	DF	RAND	10.78%	31.16%	37.73%	43.58%	45.47%
	NN	DF	3.88%	15.84%	23.48%	29.53%	33.60%
	NN	NN	3.65%	9.50%	11.22%	12.33%	12.66%
	NN	RAND	8.92%	21.38%	28.91%	34.51%	37.64%
	RAND	DF	9.17%	19.76%	27.89%	32.86%	36.57%
	RAND	NN	**0.00%**	0.70%	**0.00%**	0.13%	0.49%
	RAND	RAND	19.17%	34.10%	41.63%	46.38%	48.68%

The performance of strategies combinations is expressed relative to the strategies combination that performed with the shortest mean DC cycle time in a given AVS/RS configuration. Furthermore, for each AVS/RS configuration, parameter η_{area} was calculated that enable comparison of space area utilisation.

Low occupancy

The shortest mean DC cycle time for a low occupancy ($\alpha = 60\%$) is achieved with a 'NN storage and NN relocation' assignment strategies combination for a double and a triple-deep AVS/RS. Next, in the case of a fourfold, fivefold and sixfold AVS/RS, 'DF storage and NN relocation', assignment strategies combination gives us the shortest mean DC cycle times.

The 'RAND storage and NN relocation' assignment strategies combination performed very well (5 % longer mean DC cycle time compared to the best result) in deeper AVS/RS (fivefold and sixfold-deep).

The highest mean DC cycle time relative to the best result is achieved with the 'RAND relocation' assignment strategy. 'RAND storage and RAND relocation' being the assignment strategies combination with the poorest performance.

Medium occupancy

At fill-grade factor ($\alpha = 75\%$), the 'NN storage and NN relocation' assignment strategies combination performed with the shortest cycle time for a double-deep AVS/RS. While for the triple, fourfold, fivefold, and sixfold-deep AVS/RS, 'DF storage and NN relocation' assignment strategies combination performed with the shortest DC cycle time.

The 'RAND storage and NN relocation' assignment strategies combination again performed very well (less than 5 % longer mean DC cycle time, compared to the best result) in the case of fourfold, fivefold and sixfold deep AVS/RS.

High occupancy

Lastly, at fill-grade factor ($\alpha = 90\%$), the relative difference in performance between 'RAND storage and NN relocation' and 'DF storage and NN relocation' assignment strategies combinations further decreases. At a high occupancy level, both strategies combination performed almost equally well (less than 3 % difference between mean DC cycle times).

As in AVS/RS with low or medium occupancy, the 'RAND storage and RAND relocation' assignment strategy combination performed with the longest relative mean DC cycle time.

5 Discussion

This paper studied multiple-deep AVS/RS with three storage and relocation assignment strategies (nearest neighbour, depth-first and random), which gives us nine (9) different strategies combinations. Mean DC cycle times for all nine (9) storage and relocation assignment strategies combinations were evaluated and compared with five (5) different multiple-deep AVS/RS configurations. The retrieval of SKUs was undetermined, meaning that no information was given about SKUs retrieval order. All of the evaluated AVS/RS had the same number of storage locations (1200) by changing the number of columns (C) and the number of depths (D). Further, we explored the impact of different occupancy levels by varying the fill-grade factor (α). The performance evaluation was accomplished with a discrete event simulation of the AVS/RS with a satellite vehicle attached to a shuttle carrier.

For a double-deep AVS/RS, with a fill-grade factor ($\alpha \leq 85\%$), a combination of 'NN storage and NN relocation' assignment strategies combination achieved the shortest mean DC cycle time. On the contrary, at a higher fill-grade factor ($\alpha = 90\%$ and $\alpha = 95\%$), the 'DF storage and NN relocation' and 'RAND storage and NN relocation' assignment strategies combination should be utilised, respectively.

At a lower fill-grade factor ($\alpha < 65\%$) in a triple-deep AVS/RS (similar to a double-deep AVS/RS) 'NN storage and NN relocation' assignment strategies combination achieved the highest throughput performance. For higher fill-grade factors (α), the 'DF storage and NN relocation' assignment strategies combination should be applied. In most cases, in fourfold, fivefold, and sixfold-deep AVS/RS, the 'DF storage and NN relocation' assignment strategies combination achieved the shortest mean DC cycle times.

The simulation results show the significance of storage and specifically relocation assignment strategies on multiple-deep AVS/RS throughput performance, where a relocation operation may occur during an SKU retrieval. The shortest mean DC cycle times in AVS/RS were achieved when the 'NN relocation' strategy was utilised.

This paper's research study was based on a numerical model with specified input parameters and is fundamental for the upcoming research work. In the future, the storage and relocation assignment policies will be studied broader by generalising the input parameters. The development of new storage and relocation assignment strategies is also desirable in the research community. Further, analytical and empirical models should be provided for different assignment strategies, as probably some would likely outperform others in various AVS/RS configurations. Our research encompasses an undetermined SKU retrieval problem, where every SKU had an equal probability of being retrieved and the sequence of retrieval was unknown. This problem becomes much more exciting and complex when a partial or complete SKU retrieval sequence is given.

6 Declarations

6.1 Funding

The authors did not receive support from any organization for the submitted work. The authors have no relevant financial or non-financial interests to disclose.

6.2 Conflicts of interest/Competing interests

The authors have no conflicts of interest to declare that are relevant to the content of this article.

6.3 Availability of data and material

Not applicable.

6.4 Code availability

The simulation (MATLAB and Simulink) code of AVS/RS is available at: https://github.com/m4r0lt/AVS-RS.

6.5 Ethics approval

Not applicable.

6.6 Consent to participate

All authors certify that they have no affiliations with or involvement in any organization or entity with any financial interest or non-financial interest in the subject matter or materials discussed in this manuscript.

6.7 Consent for publication

All authors consent to the publication of this original paper.

6.8 Authors' contributions

We are the first that directly compared the performance impact of nine (9) storage and relocation assignment strategies combinations in a multiple-deep AVS/RS. Our research includes a depth-first (storage and relocation) strategy that has not been used in any paper considering automated storage systems. The paper also shows that multiple-deep (five and sixfold-deep) AVS/RS can outperform AVS/RS with fewer depths by applying the "depth-first" storage and "nearest neighbour" relocation strategy.

7 References

[1] N. Boysen, R. de Koster, and F. Weidinger, "Warehousing in the e-commerce era: A survey," *Eur. J. Oper. Res.*, vol. 277, no. 2, pp. 396–411, Sep. 2019.

[2] B. C. Park, "Order Picking: Issues, Systems and Models," in *Warehousing in the Global Supply Chain*, vol. 9781447122, London: Springer London, 2012, pp. 1–30.

[3] C. J. Malmborg, "Conceptualizing tools for autonomous vehicle storage and retrieval systems," *Int. J. Prod. Res.*, vol. 40, no. 8, pp. 1807–1822, 2002.

[4] T. Lerher, M. Sraml, I. Potrc, and T. Tollazzi, "Travel time models for double-deep automated storage and retrieval systems," *Int. J. Prod. Res.*, vol. 48, no. 11, pp. 3151–3172, Jun. 2010.

[5] C. J. Malmborg, "Interleaving dynamics in autonomous vehicle storage and retrieval systems," *Int. J. Prod. Res.*, vol. 41, no. 5, pp. 1057–1069, 2003.

[6] X. Xu, G. Shen, Y. Yu, and W. Huang, “Travel time analysis for the double-deep dual-shuttle AS/RS,” *Int. J. Prod. Res.*, vol. 53, no. 3, pp. 757–773, 2015.

[7] T. Lerher, “Travel time model for double-deep shuttle-based storage and retrieval systems,” *Int. J. Prod. Res.*, vol. 54, no. 9, pp. 2519–2540, 2016.

[8] B. Yetkin Ekren, “Graph-based solution for performance evaluation of shuttle-based storage and retrieval system,” *Int. J. Prod. Res.*, vol. 55, no. 21, pp. 6516–6526, 2017.

[9] K. J. Roodbergen and I. F. A. Vis, “A survey of literature on automated storage and retrieval systems,” *Eur. J. Oper. Res.*, vol. 194, no. 2, pp. 343–362, 2009.

[10] G. Marchet, M. Melacini, S. Perotti, and E. Tappia, “Analytical model to estimate performances of autonomous vehicle storage and retrieval systems for product totes,” *Int. J. Prod. Res.*, vol. 50, no. 24, pp. 7134–7148, 2012.

[11] J. Carlo and I. F. A. Vis, “Int . J . Production Economics Sequencing dynamic storage systems with multiple lifts and shuttles,” vol. 140, pp. 844–853, 2012.

[12] D. Roy, A. Krishnamurthy, S. S. Heragu, and C. J. Malmborg, “Blocking Effects in Warehouse Systems With Autonomous Vehicles,” *IEEE Trans. Autom. Sci. Eng.*, vol. 11, no. 2, pp. 439–451, Apr. 2014.

[13] Z. Ning, L. Lei, Z. Saipeng, and G. Lodewijks, “An efficient simulation model for rack design in multi-elevator shuttle-based storage and retrieval system,” *Simul. Model. Pract. Theory*, vol. 67, pp. 100–116, 2016.

[14] VEREIN DEUTSCHER INGENIEURE, “VDI 2692 Shuttle-Systeme für kleine Ladeeinheiten Automated vehicle storage and retrieval systems for small unit loads,” 2015.

[15] R. Manzini, R. Accorsi, G. Baruffaldi, T. Cennerazzo, and M. Gamberi, “Travel time models for deep-lane unit-load autonomous vehicle storage and retrieval system (AVS/RS),” *Int. J. Prod. Res.*, vol. 54, no. 14, pp. 4286–4304, 2016.

[16] FEM, “FEM 9.860 Guideline / Cycle time calculation for automated vehicle storage and retrieval systems,” 2017.

[17] G. D’Antonio, M. De Maddis, J. S. Bedolla, P. Chiabert, and F. Lombardi, “Analytical models for the evaluation of deep-lane autonomous vehicle storage and retrieval system performance,” *Int. J. Adv. Manuf. Technol.*, vol. 94, no. 5–8, pp. 1811–1824, 2018.

[18] G. D’Antonio and P. Chiabert, “Analytical models for cycle time and throughput evaluation of multi-shuttle deep-lane AVS/RS,” *Int. J. Adv. Manuf. Technol.*, vol. 104, no. 5–8, pp. 1919–1936, 2019.

[19] D. Boywitz and N. Boysen, “Robust storage assignment in stack- and queue-based storage systems,” *Comput. Oper. Res.*, vol. 100, pp. 189–200, 2018.

[20] Y. Ha and J. Chae, “A decision model to determine the number of shuttles in a tier-to-tier SBS/RS,” *Int. J. Prod. Res.*, vol. 57, no. 4, pp. 963–984, 2019.

[21] Y. Wang, R. Zhang, H. Liu, X. Zhang, and Z. Liu, “Task scheduling model of double-deep multi-tier shuttle system,” *Processes*, vol. 7, no. 9, pp. 1–17, 2019.

[22] M. Eder, “An approach for a performance calculation of shuttle-based storage and retrieval systems with multiple-deep storage,” *Int. J. Adv. Manuf. Technol.*, vol. 107, no. 1–2, pp. 859–873, Mar. 2020.

[23] Y. Wang, R. Man, X. Zhao, and H. Liu, “Modeling of parallel movement for deep-lane unit load autonomous shuttle and stacker crane warehousing systems,” *Processes*, vol. 8, no. 1, 2020.

8 Appendix

Mean dual command cycle time T(DC)										
	Storage strategy	DF	DF	DF	NN	NN	NN	RAND	RAND	RAND
	Relocation strategy	DF	NN	RAND	DF	NN	RAND	DF	NN	RAND
$D = 2,\ C = 300$	$\alpha = 50\%$	80.34	80.34	80.40	57.13	**53.42**	71.13	81.80	81.55	93.56
	$\alpha = 55\%$	77.78	77.76	82.20	61.20	**57.02**	73.33	81.88	81.67	94.49
	$\alpha = 60\%$	75.92	75.91	83.66	65.32	**60.66**	75.55	82.03	81.79	95.28
	$\alpha = 65\%$	74.90	74.90	85.27	69.46	**64.45**	77.93	82.21	81.91	95.97
	$\alpha = 70\%$	74.71	74.72	85.89	73.39	**68.16**	79.80	82.38	82.06	96.47
	$\alpha = 75\%$	75.34	75.40	87.16	77.48	**71.61**	82.09	82.72	82.16	97.11
	$\alpha = 80\%$	76.91	76.86	88.39	79.55	**75.41**	84.18	83.06	82.41	97.67
	$\alpha = 85\%$	79.15	79.18	89.33	80.89	**79.11**	86.20	83.67	82.53	98.55
	$\alpha = 90\%$	81.99	**81.94**	90.80	83.28	82.68	88.67	84.90	82.85	98.78
	$\alpha = 95\%$	85.42	85.44	92.33	86.57	86.38	90.78	90.98	**83.34**	99.32
$D = 3,\ C = 200$	$\alpha = 50\%$	57.06	53.56	65.39	59.42	**47.30**	66.44	62.85	61.80	78.15
	$\alpha = 55\%$	58.96	53.18	67.29	59.26	**49.93**	68.18	64.78	62.02	79.27
	$\alpha = 60\%$	61.84	53.42	69.19	59.43	**52.56**	69.21	69.69	62.28	80.84
	$\alpha = 65\%$	65.61	**54.01**	71.15	60.58	55.24	70.80	71.76	62.45	81.83
	$\alpha = 70\%$	71.05	**55.12**	73.19	62.38	57.85	72.11	72.78	62.72	82.60
	$\alpha = 75\%$	69.97	**56.49**	75.53	64.83	60.42	73.37	72.98	63.09	83.79
	$\alpha = 80\%$	69.04	**58.20**	78.38	68.08	63.12	74.66	73.02	63.37	85.17
	$\alpha = 85\%$	68.64	**60.17**	80.53	71.22	65.83	76.08	73.50	63.85	85.27
	$\alpha = 90\%$	69.04	**62.32**	83.50	72.77	68.46	77.21	73.86	64.37	85.93
	$\alpha = 95\%$	71.18	**64.88**	85.10	75.16	71.05	78.76	77.70	65.34	87.01
$D = 4,\ C = 150$	$\alpha = 50\%$	60.13	**46.01**	60.81	53.03	46.22	64.84	61.06	53.28	72.11
	$\alpha = 55\%$	58.80	**47.17**	63.32	55.21	48.32	66.03	61.60	53.64	73.86
	$\alpha = 60\%$	58.36	**48.75**	66.42	58.18	50.46	67.39	61.97	53.99	75.43
	$\alpha = 65\%$	58.39	**50.53**	69.59	61.07	52.67	68.90	62.60	54.39	76.90
	$\alpha = 70\%$	59.89	**52.56**	72.63	61.78	54.76	70.09	66.48	54.82	77.81
	$\alpha = 75\%$	70.44	**53.42**	75.01	62.74	56.87	71.30	70.20	55.35	79.19
	$\alpha = 80\%$	69.74	**54.08**	76.76	64.60	58.94	72.21	71.41	55.82	80.12
	$\alpha = 85\%$	68.83	**55.22**	77.90	67.59	61.11	73.39	71.68	56.43	81.40
	$\alpha = 90\%$	68.11	**57.15**	79.26	70.85	63.27	74.53	72.21	57.21	82.74
	$\alpha = 95\%$	68.51	59.74	80.98	72.60	65.40	75.80	75.20	**58.80**	83.28
$D = 5,\ C = 120$	$\alpha = 50\%$	52.41	**45.38**	61.34	56.07	47.44	65.20	56.53	49.55	70.40
	$\alpha = 55\%$	53.75	**47.46**	64.71	56.79	49.35	66.36	59.87	50.05	72.29
	$\alpha = 60\%$	62.76	**48.49**	67.77	57.65	51.24	68.12	63.29	50.54	73.92
	$\alpha = 65\%$	62.39	**49.01**	70.22	59.90	53.13	69.33	64.27	51.05	75.34
	$\alpha = 70\%$	61.95	**49.53**	72.32	62.90	54.86	70.62	64.64	51.62	76.87
	$\alpha = 75\%$	61.99	**50.10**	74.00	64.63	56.62	71.88	66.96	52.35	78.17
	$\alpha = 80\%$	72.09	**51.17**	76.02	66.06	58.37	72.84	71.74	53.08	79.73
	$\alpha = 85\%$	71.63	**52.54**	77.49	68.07	60.36	74.42	72.66	53.86	80.78
	$\alpha = 90\%$	70.56	**54.53**	79.67	71.73	62.06	74.87	73.58	54.98	81.89
	$\alpha = 95\%$	70.86	**56.82**	81.58	73.59	63.82	76.42	75.49	56.89	83.17
$D = 6,\ C = 100$	$\alpha = 50\%$	58.55	**46.14**	63.77	55.59	49.94	66.63	59.17	48.36	70.50
	$\alpha = 55\%$	57.99	**46.70**	66.49	58.04	51.75	68.32	60.48	48.91	72.55
	$\alpha = 60\%$	58.26	**47.12**	68.87	61.08	53.29	70.00	61.77	49.53	74.66
	$\alpha = 65\%$	60.30	**47.76**	70.94	62.24	54.94	71.28	66.38	50.17	76.49
	$\alpha = 70\%$	66.97	**48.73**	73.73	64.18	56.58	73.26	68.18	51.12	78.36
	$\alpha = 75\%$	66.69	**49.82**	75.77	67.10	58.01	73.94	68.98	51.91	79.76
	$\alpha = 80\%$	67.14	**51.11**	78.53	69.17	59.77	75.58	71.93	52.78	80.93
	$\alpha = 85\%$	75.18	**52.64**	80.00	70.95	61.44	76.66	76.18	53.83	83.08
	$\alpha = 90\%$	74.40	**54.46**	82.18	73.87	62.75	77.50	76.87	55.09	83.87
	$\alpha = 95\%$	74.31	**57.36**	83.44	76.63	64.62	78.95	78.33	57.64	85.28